Kinetic Monte Carlo Simulations of the Loading Dependence of Diffusion in Zeolites

By *R. Krishna** and *J. M. van Baten*

Kinetic Monte Carlo (KMC) simulations are used to model diffusion of molecules in zeolites. A variety of loading dependences of the Maxwell-Stefan diffusivity, $Đ_i$, can be realized by allowing the jump frequencies, ν, of molecules to be influenced by the presence of neighboring molecules. Neighboring molecules are assumed to reduce or increase the activation energy for diffusion by δE and the jump frequencies ν are altered by a factor $f = \exp(\delta E/RT)$ for each neighboring molecule. By appropriate choice of ν and f the loading dependence of $Đ_i$ can be made to match those obtained from either Molecular Dynamics (MD) simulations or experiment. The major advantage of the KMC simulation strategy is that considerably less computer power is required than for the corresponding MD simulations. Furthermore, KMC simulations allow mixture diffusion to be probed without additional parameter tuning. The KMC simulations also validate the applicability of the quasi-chemical theory of Reed and Ehrlich (*Surf. Sci.* **1981**, *105*, 603–628) for describing the loading dependence of $Đ_i$.

1 Introduction

Zeolites are crystalline nanoporous materials that are widely used in the chemical industry as catalysts and adsorbents [1–3]. Zeolite crystals are incorporated into binders and used in the form of pellets in fixed or simulated moving bed reactors. Alternatively, zeolite crystals are coated on to a porous membrane support and used in (catalytic) membrane reactors and separation devices [4]. More than 100 different zeolite structures are encountered in practice [5]. Viewed simply, these structures fall into three broad categories, (a) structures with intersecting channels (examples include MFI, MEL, BOG), (b) cages separated by windows (LTA, FAU), and (c) essentially one-dimensional channels (AFI, MTW), sometimes with side pockets (MOR).

In the development of separation and reaction processes using zeolites, the proper description of diffusion of molecules within zeolites is an essential step and it is generally accepted that the Maxwell-Stefan (M-S) diffusion formulation provides a convenient and general framework that can be used in practice [6–8]. For single component diffusion of species i, the M-S formulation[1)]

$$N_i = -\rho\Theta_i Đ_i \frac{1}{RT}\nabla\mu_i \equiv -\rho\Theta_{i,sat} Đ_i \frac{\theta_i}{RT}\nabla\mu_i \qquad (1)$$

relates the flux N_i to the chemical potential gradient $\nabla\mu_i$. In Eq. (1), Θ_i is the molecular loading expressed say in molecules per unit cell, $\Theta_{i,sat}$ is the saturation loading, $\theta_i \equiv \Theta_i/\Theta_{i,sat}$ is the fractional occupancy, ρ is the zeolite framework density expressed as the number of unit cells per m^3, R is the gas constant, T is the temperature, and $Đ_i$ is the M-S diffusivity.

Both Molecular Dynamics (MD) simulations [9, 10] and experimental studies with MFI zeolite [11–14] have revealed a wide variety of dependencies of the Maxwell-Stefan diffusivity, $Đ_i$, on the loading Θ_i. The important advantage of MD simulations is that with the appropriate choice of the force field it is possible to obtain the correct estimate of both the magnitude of $Đ_i$ and its dependence on the loading Θ_i [11, 12]. However, MD simulations are computationally very demanding. Kinetic Monte Carlo (KMC) simulations [6, 15] demand much less computer power but do not possess the predictive power of MD simulations. The jump frequencies of molecules, ν_i, need to be supplied as inputs to KMC simulations; these can be estimated from the transition state theory [16] or MD simulations [6, 15, 17]. Using the standard KMC simulation strategy the occupancy dependence of $Đ_i$ invariably follows the dependence

$$Đ_i = Đ_i(0)\left(1 - \theta_i\right) \qquad (2)$$

Eq. (2) was found to hold for example for 2-methylhexane (2MH) in MFI [17]. In order to reproduce the wide variety of observed loading dependences other than that portrayed by Eq. (2) it is necessary to allow the jump frequencies to be influenced by each of the neighboring molecules by a factor $f = \exp(\frac{\delta E}{RT})$, where δE represents the reduction in the energy barrier, following the KMC simulation strategy as described elsewhere [18–21] and the details are not repeated here.

The first major objective of the present communication is to show the KMC simulations can be properly *tuned* to reproduce either MD or experimental $Đ_i - \Theta_i$ data. Secondly, we also demonstrate that the KMC data verify the model of Reed and Ehrlich [22], appropriately generalized as follows [19]:

$$Đ_i(\theta) = Đ_i(0)\frac{(1+\varepsilon)^{z-1}}{(1+\varepsilon/f)^z} \qquad (3)$$

[*] R. Krishna (author to whom correspondence should be addressed, R.Krishna@uva.nl), J. M. van Baten, Van't Hoff Institute for Molecular Sciences, University of Amsterdam, Nieuwe Achtergracht 166, 1018 WV Amsterdam, The Netherlands.

1) List of symbols at the end of the paper.

  DOI: 10.1002/ceat.200407094

where z is the coordination number, representing the maximum number of nearest neighbors and the other parameters are given by

$$f = \exp(\frac{\delta E}{RT}); \quad \varepsilon = \frac{(\beta - 1 + 2\theta)f}{2\,(1-\theta)};$$

$$\beta = \sqrt{1 - 4\,\theta(1-\theta)(1-1/f)} \tag{4}$$

The Reed-Ehrlich model provides a convenient mean-field approach to modeling the occupancy dependence of $Đ_i$ that can be used for engineering purposes.

The final objective is to demonstrate that if individual species in a mixture are tuned in this manner, KMC simulations can be used to probe the mixture diffusion characteristics with considerably less computer power than the corresponding MD simulations.

2 Single Component Diffusion in Various Topologies

Let us first consider diffusion in square and cubic lattices for which the coordination numbers are z = 4 and 6, respectively. The KMC simulations of the M-S diffusivity, normalized with respect to the zero-loading diffusivity, $Đ_i/Đ_i(0)$ for square and cubic lattices are shown by open symbols in Figs. 1a, b for varying values of the factor f = 0.5, 1, 1.5, and 2. Also shown with continuous solid lines in Figs. 1a, b are the corresponding calculations using the Reed-Ehrlich model, Eq. (3). The agreement between the KMC simulations and the Reed-Ehrlich model is perfect as expected, because the KMC simulations were set up using exactly the same physical model underlying the Reed-Ehrlich development.

Now let us turn to diffusion of 2-methylhexane (2MH) in MFI zeolite at 300 K. From configurational considerations this branched alkane can only be located at the intersections between the straight (st) and zig-zag (zz) channels [23]; see Fig. 2. The saturation capacity is therefore $\Theta_{i,sat}$ = 4 molecules per unit cell and so we take the total number of adsorption sites as 4, all located at the intersections. The jump frequencies of 2MH along the straight channels, ν_{st}, and zig-zag channels, ν_{zz}, can be estimated using the transition state theory [24] and are specified in Tab. 1. The KMC simulation results are shown by the open symbols in Fig. 3a for f = 0.5, 1, 1.5, and 2. The continuous solid lines in Fig. 3a are the calculations using the Reed-Ehrlich model, Eq. (3), taking z = 4. The choice of the coordination number is dictated by the fact that each molecule at the intersections has four neighboring molecules, also located at the intersections.

The corresponding KMC simulations of the *self*-diffusivity of 2MH in MFI are shown in Fig. 3a for f = 0.5, 1, 1.5 and 2. The continuous solid lines in Fig. 3a were obtained from

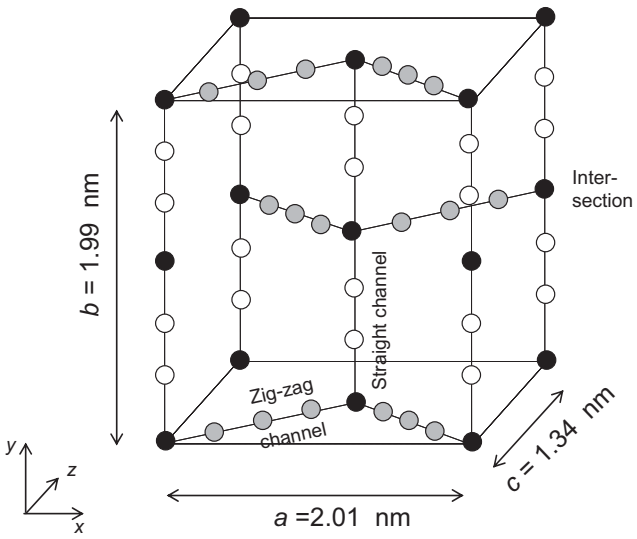

Figure 2. Unit cell for MFI lattice topology with a total of 24 sites per unit cell; these sites are indicated as black circles (intersections), white circles (straight channels) and grey circles (zig-zag channels). The distribution of the 24 molecules per unit cell is as follows: 4 at intersections, 8 within straight channels, and 12 within the zig-zag channels.

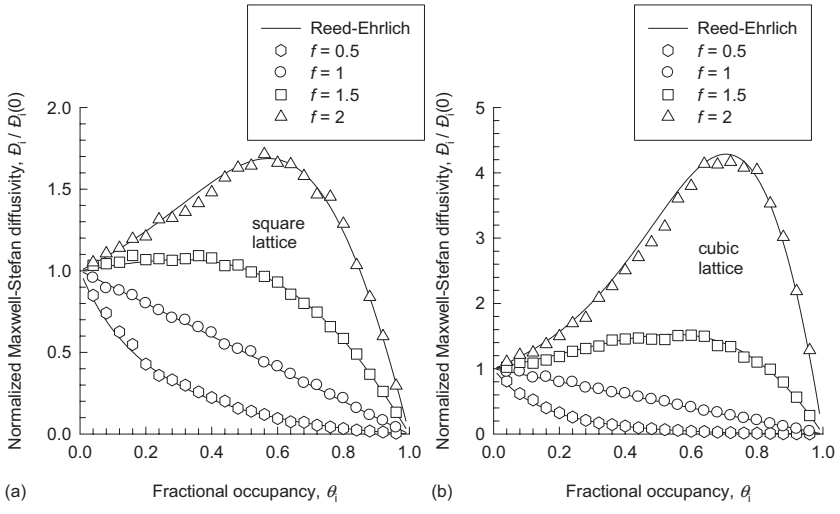

Figure 1. KMC simulations (open symbols) of normalized M-S diffusivity, $Đ_i/Đ_i(0)$ in (a) square, and (b) cubic lattice topologies. Also shown using continuous solid lines are the calculations of $Đ_i/Đ_i(0)$ with the Reed-Ehrlich model, Eq. (3).

Table 1. Model parameters for various molecules in MFI zeolite. The temperatures are in degrees K. The jump frequencies ν_{st} and ν_{zz} have the unit s^{-1}. The zero-loading M-S diffusivities $Đ_i(0)$ have the units of $m^2\ s^{-1}$. The other parameters a_1 and a_2 are dimensionless.

Molecule	Temperature	Number of sites	ν_{st}	ν_{zz}	z	$Đ_i(0)$	$Đ_{ii}/Đ_i = a_1 \exp(-a_2\theta)$	
							a_1	a_2
2MH	300	4	1.4×10^5	5×10^4	4	6.7×10^{-14}	1.4	0.5
3MP	423	4	2.8×10^6	1×10^6	4	1.35×10^{-12}	1.4	0.5
N_2	200	20	2.2×10^{11}	1.1×10^{11}	2.4	0.8×10^{-8}	0.7	1.2
CO_2	300	24	2×10^{11}	1×10^{11}	2.33	0.55×10^{-8}	0.5	0.9
CH_4	298	20	4×10^{11}	2×10^{11}	2.4	1.45×10^{-8}	0.7	1.2
CF_4	298	20	1.2×10^{11}	7×10^{10}	2.4	0.47×10^{-8}	0.7	1.2

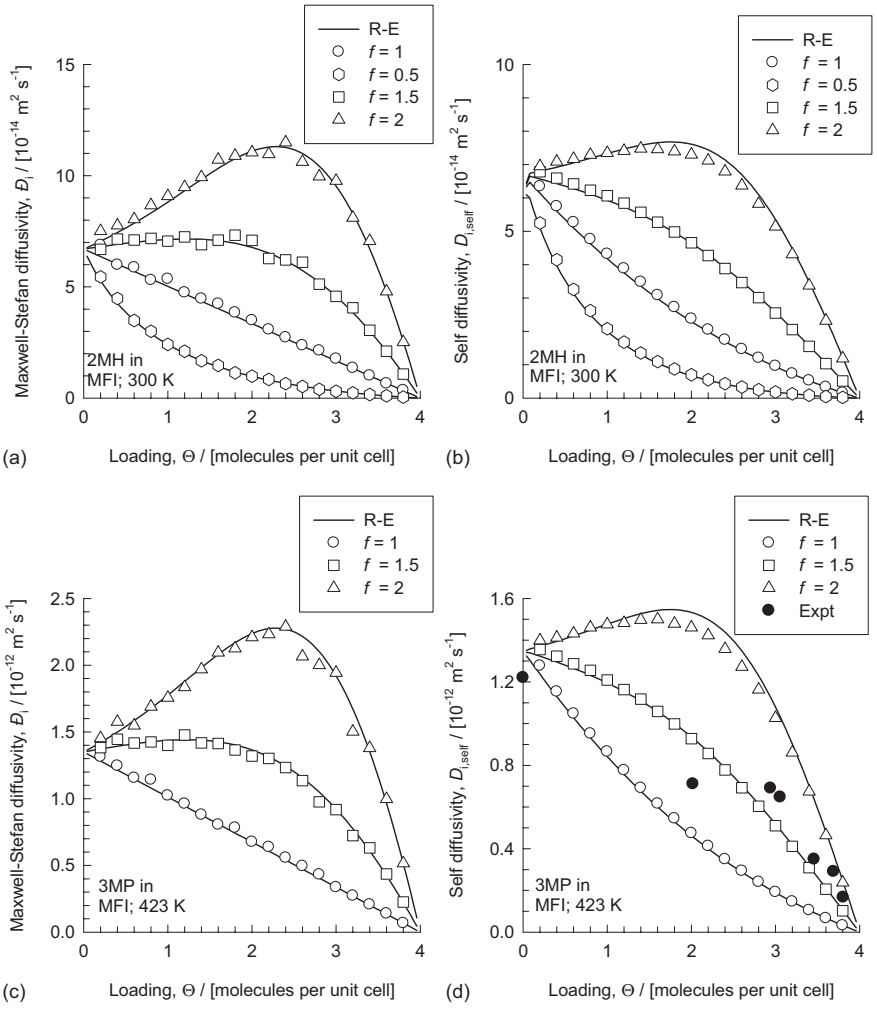

Figure 3. KMC simulations (open symbols) of M-S diffusivity $Đ_i$ and self diffusivity $Đ_{i,self}$ in MFI of (a, b) 2MH at 300 K, and (c, d) 3MP at 423 K. Also shown using continuous solid lines are the calculations of $Đ_i$ with the Reed-Ehrlich model, Eq. (3). The filled black circles in (d) represent the experimental values reported by Koriabkina *et al.* [13].

calculations using the following formula for the self-diffusivity, $D_{i,self}$

$$D_{i,self} = \frac{1}{\frac{1}{Đ_i} + \frac{\theta_i}{Đ_{ii}}} \tag{5}$$

where $Đ_{ii}$ is the *self-exchange* coefficient that arises naturally in the M-S formulation for tracer diffusion of a labeled species in an environment of unlabeled species [8]. The parameter $Đ_{ii}/Đ_i$, can be taken as a measure of correlation effects. The lower the value of $Đ_{ii}/Đ_i$, the stronger the influence of correlations. A very large value of $Đ_{ii}/Đ_i$ signifies weak correlations between molecular jumps. The $Đ_{ii}/Đ_i$ is also occupancy dependent and this dependence can be generally described by

$$\frac{Đ_{ii}}{Đ_i} = a_1 \exp\left(-a_2\ \theta_i\right) \tag{6}$$

following the work of Skoulidas *et al.* [8]. For the 2MH diffusion in MFI the parameters a_1 and a_2 were chosen as 1.4 and 0.5. The good agreement between Eq. (5) and the KMC simulations for a variety of values of the interaction parameter implies that the self-exchange coefficient is *not* influenced by the chosen value for *f*. This is a useful simplification to the description of diffusion in mixtures, in which $Đ_{ii}$ plays a crucial role [8].

Koriabkina *et al.* [13] report experimental data on the loading dependence of the self-diffusivity of 3-methylpentane (3MP) in MFI at 423 K. We try to rationalize the experimentally observed loading dependence by performing KMC simulations of both $Đ_i$ and $D_{i,self}$ for a variety of values of *f*; the results are shown by the open symbols in Figs. 3c, d. In performing these simulations the ratio of the jump frequencies ν_{st}/ν_{zz}, was taken to be the same as that for 2MH in MFI and their absolute values (see

Tab. 1) were tuned to match the zero-loading diffusivity value $Đ_i(0) = 1.35\times10^{-12}$ m^2 s^{-1} obtained in the experiments.

The filled black circles in Fig. 3d representing the experimental data on $D_{i,self}$ correspond to the KMC simulations taking $f = 1.5$. The experimental data on the loading dependence can be rationalized if we take the energy barrier for diffusion of 3MP in MFI to be reduced due to increased loading. The Reed-Ehrlich model, taking $z = 4$, provides an accurate mean-field model for the KMC simulation results of $Đ_i$ for all values of f. Furthermore Eqs. (5) and (6), with $a_1 = 1.4$ and $a_2 = 0.5$ provide an excellent description of the KMC simulations of the self-diffusivity.

In Fig. 4a we present the KMC simulation results of the M-S diffusivity $Đ_i$ of N_2 in MFI at $T = 200$ K. The jump frequencies, specified in Tab. 1, were tuned to match the zero-loading diffusivity $Đ_i(0) = 0.8\times10^{-8}$ m^2 s^{-1} obtained in the MD simulations reported by Papodopoulos *et al.* [12]. The number of sorption sites per unit cell was taken to be 20 on the basis of the sorption isotherm data [12]. The loading dependence of $Đ_i$ for N_2 obtained from their MD data can be rationalized by KMC simulations taking $f = 1.9$. In order to perform the calculations with the Reed-Ehrlich model we also need to specify the coordination number z. For N_2 we have a total of 20 sorption sites, of which 4 are located at the intersections. Each of the intersection sites sees a maximum of 4 neighbors. The other 16 sites are located in the channel interiors, 8 each in the straight and zig-zag channels. A channel site sees only 2 neighboring molecules. Therefore the average coordination number z can be calculated as $z = (16\times2+4\times4)/20 = 2.4$. The continuous lines in Fig. 4a are the Reed-Ehrlich model calculations taking $z = 2.4$ and the corresponding f value chosen for the KMC simulations. The agreement with the KMC simulations is excellent.

In Fig. 4b we present the KMC simulation results of the M-S diffusivity $Đ_i$ of CO_2, in MFI at $T = 300$ K. The jump frequencies, specified in Tab. 1, were tuned to match the zero-loading diffusivity $Đ_i(0) = 0.55\times10^{-8}$ m^2 s^{-1} obtained in the MD simulations reported by Papodopoulos *et al.* [12]. The number of sorption sites per unit cell was taken to be 24 on the basis of the sorption isotherm data [12]. The loading dependence of $Đ_i$ for CO_2 obtained from their MD data can be rationalized by KMC simulations taking $f = 0.9$. In order to perform the calculations with the Reed-Ehrlich model we also need to specify the coordination number z. For CO_2 we have a total of 24 sorption sites, of which 4 are located at the intersections. Each of the intersection sites sees a maximum of 4 neighbors. The other 20 sites are located in the channel interiors; 8 in the straight channels and 12 within the zig-zag channels as shown in Fig. 2. As before the average coordination number can be calculated from $z = (20\times2+4\times4)/20 = 2.33$. The continuous lines in Fig. 4b are the Reed-Ehrlich model calculations taking $z = 2.33$ and the corresponding f value chosen for the KMC simulations. The agreement with the KMC simulations is again excellent.

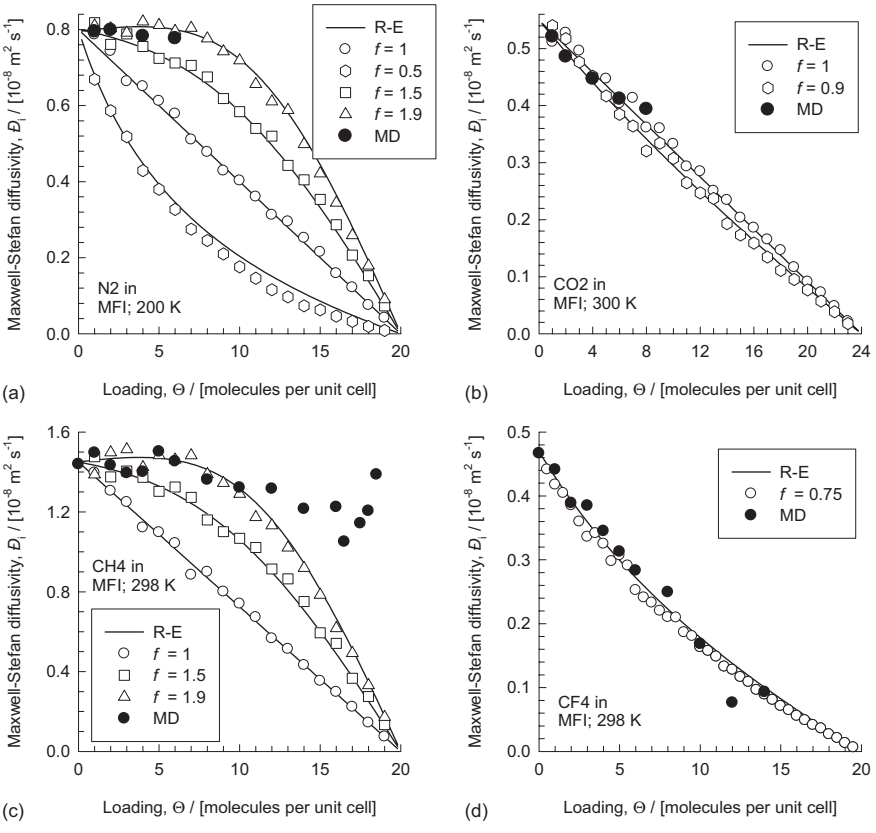

Figure 4. KMC simulations (open symbols) of M-S diffusivity $Đ_i$ in MFI of (a) N_2 at 200 K, (b) CO_2 at 300 K, (c) CH_4 at 298 K, and (d) CF_4 at 298 K. Also shown using continuous solid lines are the calculations of $Đ_i$ with the Reed-Ehrlich model, Eq. (3). The filled black circles represent the MD simulation results [8, 12].

Let us now consider the KMC simulations for diffusion of CH_4 in MFI at 298 K. From the sorption isotherm data we take the number of sorption sites per unit cell to be 20 [8]. The jump frequency along the straight channels is taken as $\nu_{str} = 4\times10^{11}$ s^{-1}; for transport along the zig-zag channels we take $\nu_{zz} = 2\times10^{11}$ s^{-1}. These jump frequency values are chosen so as to match the zero-loading diffusivity $Đ_i(0) = 1.45\times10^{-8}$ m^2 s^{-1}, in the x, y and z directions, obtained from MD [8]. The number of sorption sites within the MFI lattice is taken to be 20 per unit cell (4 at intersections, 8 within straight channels, and 12 within the zig-zag channels). Simulations have been carried out taking the pair interaction factors $f = 1$, 1.5, and 1.9. The KMC results for $Đ_i$ are presented as open symbols in Fig. 4c. Up to a loading Θ_i of 10, the MD results (filled black circles) can be matched

with the KMC simulations taking f = 1.9. The continuous lines in Fig. 4c represent calculations of the Reed-Ehrlich model taking z = 2.4, a value calculated above for N_2 with a total of 20 sorption sites.

Let us now consider the KMC simulations for diffusion of CF_4 in MFI at 298 K. We take the number of sorption sites per unit cell to be 20, despite the fact that the sorption isotherm indicates a maximum of 16 [8]; the reason for choosing 20 sites is that we later wish to simulate diffusion of a mixture of CH_4 and CF_4. In KMC simulations of mixtures, to be described later, it is not possible to cope with different number of sorption sites for the constituent species. The jump frequency along the straight channels is taken as ν_{str} = 1.2×10^{11} s^{-1}; for transport along the zig-zag channels we take ν_{zz} = 7×10^{10} s^{-1}. These jump frequency values are chosen so as to match the zero-loading diffusivity $Đ_i(0)$ = 0.47×10^{-8} m^2 s^{-1}, in the x, y and z directions, obtained from MD [8]. The MD results (filled black circles) can be matched with the KMC simulations taking f = 0.75; see Fig. 4d. The continuous lines in Fig. 4d represent calculations of the Reed-Ehrlich model taking z = 2.4; the agreement with KMC simulations is excellent.

For diffusion of CH_4 in the one-dimensional channels of MTW (ZSM-12), the M-S diffusivity $Đ_i$ shows a slight inflection at a loading of 7 molecules per unit cell [9]; see Fig. 5a. This inflection is caused by the isotherm inflection, shown in Fig. 5b. The continuous lines in Fig. 5b represent the dual-site Langmuir isotherm

$$\Theta(p) \equiv \Theta_A + \Theta_B = \frac{\Theta_{sat,A} b_A p}{1+b_A p} + \frac{\Theta_{sat,B} b_B p}{1+b_B p} \quad (7)$$

where the saturation capacities Θ_{sat} of sites A (strong) and B (weak) are 7 and 5 molecules per unit cell, respectively. The corresponding Langmuir parameters are b_A = 1.29×10^{-6} Pa^{-1} and b_B = 8.65×10^{-9} Pa^{-1}. The KMC simulations of $Đ_i$ (for topological details see [21]) taking the jump frequencies ν = 4×10^{11} s^{-1} are shown by the open symbols in Fig. 5a. To capture the inflection behavior of $Đ_i$ we take the jump frequencies *away* from the weak sites B to be a factor b_A/b_B = 150 higher than the jump frequencies *towards* the weak sites, a KMC strategy explained in our earlier publication [10]. With this strategy the inflection in $Đ_i$ occurs at Θ = 7, faithful to the MD simulations. The continuous line in Fig. 5a is the extension of the scenario described by Eq. (2), derived earlier [10]:

$$Đ = Đ(0)\,[x_A\,(1-\Theta_A/\Theta_{sat,A}) + x_B\,(1-\Theta_B/\Theta_{sat,B})] \quad (8)$$

where we take $Đ(0)$ = 6×10^{-8} m^2 s^{-1}. A similar loading dependence of $Đ_i$ is found for diffusion of CH_4 in the one dimensional channels of AFI as evidenced by the MD simulations results [25] (filled black circles), which show an inflection at a loading of 8 molecules per unit cell; see Fig. 5c. The KMC simulations of $Đ_i$ (for topological details see [21]) taking the jump frequencies ν = 1.4×10^{12} s^{-1} are shown by the open symbols in Fig. 5c. To capture the inflection behavior of $Đ_i$ we take the jump frequencies *away* from the weak sites B, four in number, to be a factor b_A/b_B = 270 higher than the jump frequencies *towards* the weak sites where the values b_A = 5.51×10^{-4} Pa^{-1} and b_B = 2.05×10^{-6} Pa^{-1} are obtained from GCMC simulations. The continuous line in Fig. 5c is the scenario described by Eq. (8), where we take $Đ(0)$ = 6×10^{-8} m^2 s^{-1}.

For diffusion of CH_4 in the cage structure of LTA (zeolite 5A), with *narrow* windows separating the cages, the M-S diffusivity $Đ_i$ shows a strong increase with loading, due to the reduction of the diffusion of the energy barrier [26]; see the black filled circles in Fig. 6a. KMC simulations (for topological details see [21]) can be made to reproduce the loading dependence by taking the rate limiting *inter*cage jump frequency to be ν = 2×10^9 s^{-1} and the factor f = 2; see the open symbols in Fig. 6a. The continuous solid lines represent the

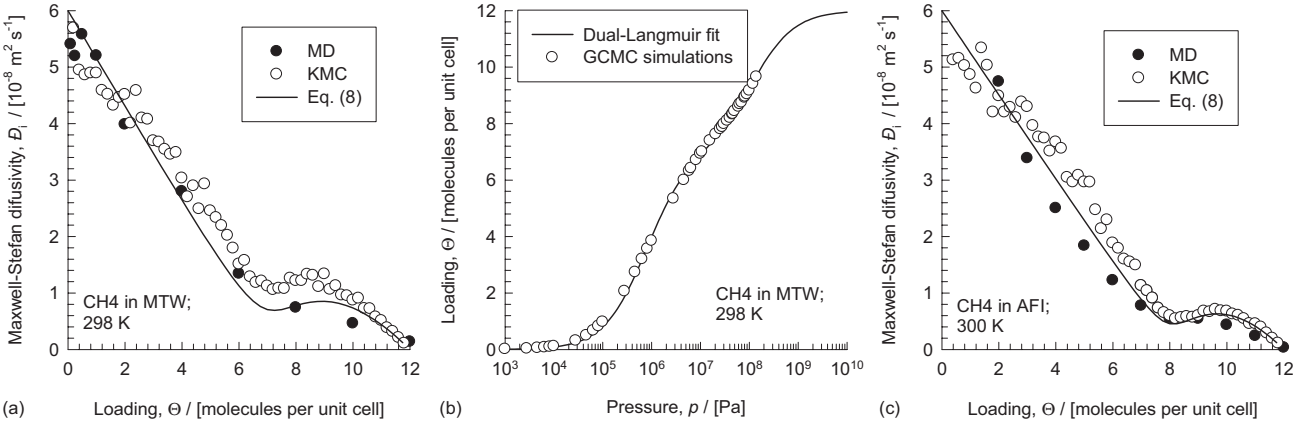

Figure 5. (a) KMC simulations (open symbols) of M-S diffusivity $Đ_i$ of CH_4 in MTW at 298 K. Also shown using continuous solid lines are the calculations of $Đ_i$ using Eq. (8). The filled black circles represent the MD simulation results [9]. (b) GCMC simulations [9] of the isotherm for CH_4 in MTW at 298 K. The continuous lines represent the dual-site Langmuir fits using Eq. (7). (c) KMC simulations (open symbols) of M-S diffusivity $Đ_i$ of CH_4 in AFI at 300 K. Also shown using continuous solid lines are the calculations of $Đ_i$ using Eq. (8). The filled black circles represent the MD simulation results [25].

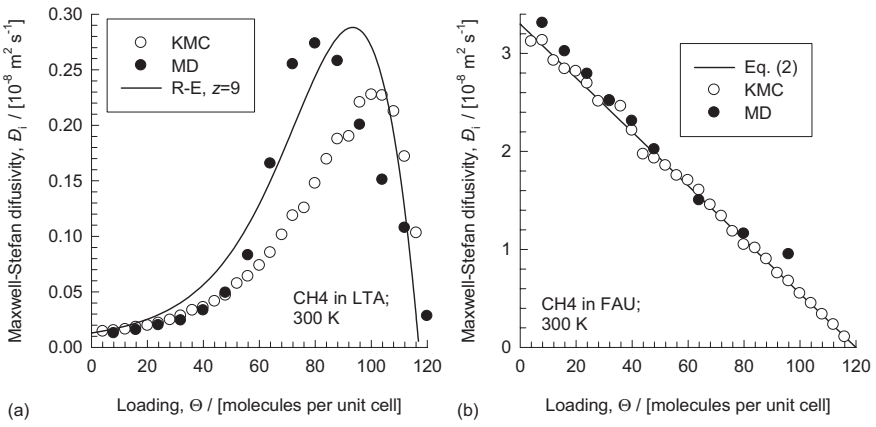

Figure 6. (a) KMC simulations (open symbols) of M-S diffusivity $Đ_i$ of CH_4 in LTA at 300 K. The filled black symbols represent the MD simulation results of Beerdsen *et al.* [26]. Also shown using continuous solid lines are the calculations of $Đ_i$ with the Reed-Ehrlich model, Eq. (3), taking $z = 9$. (b) KMC simulations (open symbols) of M-S diffusivity $Đ_i$ of CH_4 in FAU at 300 K. The filled black symbols represent the MD simulation results of Chempath *et al.* [27]. Also shown using continuous solid lines are the calculations of $Đ_i$ using Eq. (2).

Reed-Ehrlich model taking $f = 2$ and $z = 9$. The value of the coordination number is dictated by the fact that each of the 15 sorption sites within a cage is connected with 9 neighboring sites for jumps.

A different loading dependence is found for diffusion of CH_4 in the cage structure of FAU wherein the cages are separated by *large* windows; witness the MD simulation results of Chempath *et al.* [27], shown by the black filled circles in Fig. 6b. The KMC simulations (for topological details see [21]) can be made to reproduce the loading dependence by taking the rate jump frequency to be $\nu = 9.5\times10^{11}$ s^{-1}; see the open symbols in Fig. 6b. The continuous solid lines in Fig. 6b represent calculations according to Eq. (2).

3 Mixture Diffusion

Skoulidas *et al.* [28] have reported MD simulations for a mixture of CH_4 and CF_4 in MFI zeolite at 298 K. From their data the following modified matrix of $[\Lambda]$ of Onsager diffusivities, defined by

$$(N) = -\rho\Theta_{sat}\,[\Lambda]\frac{1}{RT}(\nabla\mu) \tag{9}$$

can be determined wherein we take $\Theta_{sat} = 20$ molecules per unit cell; these simulation results are shown by the filled black symbols in Figs. 7a, b, c, and d for mixtures with 75 %, 50 %, 30 % and 20 % methane, respectively.

The corresponding KMC simulation results, with the inputs as obtained from tuning *pure* component MD data and listed in Tab. 1 are shown by the open symbols. We note that the KMC simulations are able to match the MD data very well for all four mixture compositions for the whole range of loadings. The continuous lines in Fig. 7 represent the predictions of the M-S mixture model [8, 19, 27]

$$\begin{bmatrix}\Lambda_{11} & \Lambda_{12}\\ \Lambda_{21} & \Lambda_{22}\end{bmatrix} = \begin{bmatrix}\frac{1}{Đ_1}+\frac{\theta_2}{Đ_{12}} & -\frac{\theta_1}{Đ_{12}}\\ -\frac{\theta_2}{Đ_{21}} & \frac{1}{Đ_2}+\frac{\theta_1}{Đ_{21}}\end{bmatrix}^{-1}\begin{bmatrix}\theta_1 & 0\\ 0 & \theta_2\end{bmatrix} \tag{10}$$

The Reed-Ehrlich formula is used for the estimation of the pure component $Đ_i$ and the binary exchange coefficients $Đ_{ij}$ are estimated from the pure component self-exchange coefficients $Đ_{ii}$ and $Đ_{jji}$ by the interpolation formula developed earlier [8, 19, 27]

$$\Theta_{j,sat}Đ_{ij} = \left[\Theta_{j,sat}Đ_{ii}\right]^{\Theta_i/\left(\Theta_i+\Theta_j\right)}$$

$$\left[\Theta_{i,sat}Đ_{jj}\right]^{\Theta_j/\left(\Theta_i+\Theta_j\right)} = \Theta_{i,sat}Đ_{ji} \tag{11}$$

with the additional simplification here that the saturation capacities of the individual species are taken to be the same (= 20). The M-S mixture model also does a very good job of predicting the mixture diffusion characteristics.

4 Conclusions

In this study we have shown that the KMC simulations can be tuned to reproduce the loading dependences of the M-S diffusivity $Đ_i$ observed by MD simulations or experiments in various zeolite topologies. By allowing the jump frequencies, ν, of molecules to be influenced altered by a factor $f = \exp(\frac{\delta E}{RT})$ for each neighboring molecule a variety of loading dependences can be realized. Furthermore, KMC

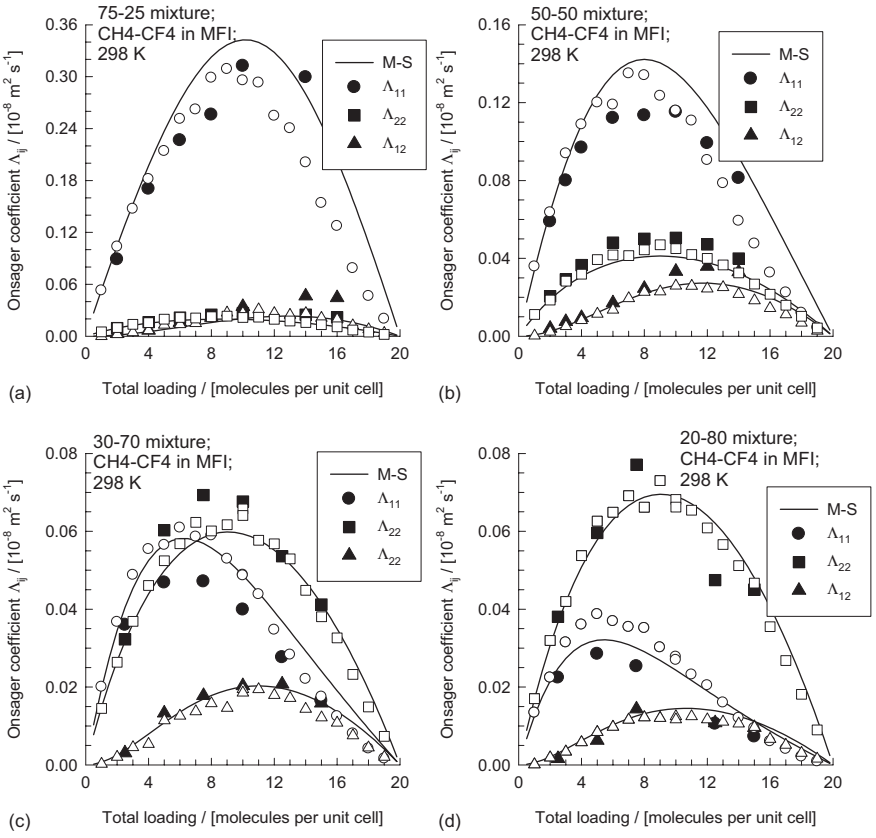

Figure 7. MD simulations (filled symbols) of Onsager matrix [Λ] for 75–25, 50–50, 30–70, and 20–80 mixtures of CH_4/CF_4 in MFI at 298 K compared with KMC simulations (open symbols). The continuous solid lines represent calculations from the M-S mixture model, with pure component parameter values are specified in Tab. 1.

simulations allow mixture diffusion to be probed without additional parameter tuning.

The KMC simulations also validate the applicability of the quasi-chemical theory of Reed and Ehrlich [22] for describing the loading dependence of $Đ_i$.

Acknowledgement

The authors acknowledge two grants *Programmasubsidie* and TOP *subsidie* from the Netherlands Foundation for Fundamental Research (CW-NWO) for development of novel concepts in reactive separations.

Received: October 31, 2004 [CET 7094]

Symbols used

a_i	[–]	constants defined in Eq. (6)
b	[Pa^{-1}]	Langmuir adsorption constants defined in Eq. (7)
$D_{i,self}$	[$m^2\ s^{-1}$]	self-diffusivity
$Đ_i$	[$m^2\ s^{-1}$]	Maxwell-Stefan diffusivity of species *i* in zeolite
$Đ_i(0)$	[$m^2\ s^{-1}$]	zero-loading Maxwell-Stefan diffusivity of species *i* in zeolite
$Đ_{ii}$	[$m^2\ s^{-1}$]	self-exchange diffusivity
$Đ_{ij}$	[$m^2\ s^{-1}$]	binary exchange diffusivity
E	[J mol^{-1}]	activation energy for diffusion
f	[–]	parameter defined by Eq. (4)
n_i	[–]	number of molecules of species *i*
n_{sites}	[–]	number of sites in KMC simulation
N_i	[molecules $m^{-2}\ s^{-1}$]	molecular flux of species *i*
p	[Pa]	pressure
R	[J $mol^{-1}\ K^{-1}$]	gas constant
t	[s]	time
T	[K]	absolute temperature
x_A	[–]	fraction of total molecules occupying site A
z	[–]	coordination number of lattice

Greek symbols

β	[–]	parameter defined by Eq. (4)
ε	[–]	parameter defined by Eq. (4)
ν	[s^{-1}]	jump frequency

θ	[–]	fractional occupancy of component *i*
Θ	[molecules uc^{-1}]	molecular loading
Θ_{sat}	[molecules uc^{-1}]	saturation loading
$[\Lambda]$	[m^2 s^{-1}]	matrix of Onsager coefficients
μ_i	[J mol^{-1}]	molar chemical potential
ρ	[uc m^{-3}]	zeolite density

Subscripts

A	strong site
B	weak site
i,j	components in mixture
sat	referring to saturation conditions
st	referring to straight channels
zz	referring to zig-zag channels
1	component 1 in binary mixture
2	component 2 in binary mixture

References

[1] D. M. Ruthven, *Principles of Adsorption and Adsorption Processes*, John Wiley & Sons, New York **1984**.
[2] J. Kärger, D. M. Ruthven, *Diffusion in Zeolites and Other microporous Solids*, John Wiley & Sons, New York **1992**.
[3] D. M. Ruthven, S. Farooq, K. S. Knaebel, *Pressure Swing Adsorption*, VCH Publishers, New York **1994**.
[4] J. Coronas, J. Santamaria, *Top Catal.* **2004**, *29*, 29.
[5] C. Baerlocher, W. M. Meier, D. H. Olson, *Atlas of Zeolite Framework Types*, Elsevier, Amsterdam **2002**.
[6] F. J. Keil, R. Krishna, M. O. Coppens, *Rev. Chem. Eng.* **2000**, *16*, 71.
[7] R. Krishna, R. Baur, *Sep. Purif. Technol.* **2003**, *33*, 213.
[8] A. I. Skoulidas, D. S. Sholl, R. Krishna, *Langmuir* **2003**, *19*, 7977.
[9] A. I. Skoulidas, D. S. Sholl, *J. Phys. Chem. A* **2003**, *107*, 10132.
[10] R. Krishna, J. M. van Baten, D. Dubbeldam, *J. Phys. Chem. B* **2004**, *108*, 14820.
[11] H. Jobic, A. I. Skoulidas, D. S. Sholl, *J. Phys. Chem. B* **2004**, *108*, 10613.
[12] G. K. Papadopoulos, H. Jobic, D. N. Theodorou, *J. Phys. Chem. B* **2004**, *108*, 12748.
[13] A. O. Koriabkina, D. Schuring, A. M. de Jong, R. A. van Santen, *Top. Catal.* **2003**, *24*, 103.
[14] W. Zhu, A. Malekian, M. Eic, F. Kapteijn, J. A. Moulijn, *Chem. Eng. Sci.* **2004**, *59*, 3827.
[15] S. M. Auerbach, *Int. Rev. Phys. Chem.* **2000**, *19*, 155.
[16] C. Tunca, D. M. Ford, *J. Chem. Phys.* **1999**, *111*, 2751.
[17] D. Paschek, R. Krishna, *Phys. Chem. Chem. Phys.* **2000**, *2*, 2389.
[18] D. Paschek, R. Krishna, *Chem. Phys. Lett.* **2001**, *342*, 148.
[19] R. Krishna, D. Paschek, R. Baur, *Microporous Mesoporous Mat.* **2004**, *76*, 233.
[20] D. Paschek, R. Krishna, *Phys. Chem. Chem. Phys.* **2001**, *3*, 3185.
[21] J. M. van Baten, R. Krishna, *Kinetic Monte Carlo Simulation of Diffusion in Zeolites*, http://ct-cr4.chem.uva.nl/kmc/, **2004**.
[22] D. A. Reed, G. Ehrlich, *Surf. Sci.* **1981**, *102*, 588.
[23] T. J. H. Vlugt, R. Krishna, B. Smit, *J. Phys. Chem. B* **1999**, *103*, 1102.
[24] B. Smit, L. Loyens, G. Verbist, *Faraday Discuss.* **1997**, 93.
[25] E. Beerdsen, D. Dubbeldam, R. Krishna, B. Smit, *To be published*, **2005**.
[26] E. Beerdsen, D. Dubbeldam, B. Smit, *Phys. Rev. Lett.* **2005**, *93 (24)*, 248 301.
[27] S. Chempath, R. Krishna, R. Q. Snurr, *J. Phys. Chem. B* **2004**, *108*, 13481.
[28] A. I. Skoulidas, T. C. Bowen, C. M. Doelling, J. L. Falconer, R. D. Noble, D. S. Sholl, *J. Membr. Sci.* **2003**, *227*, 123.

